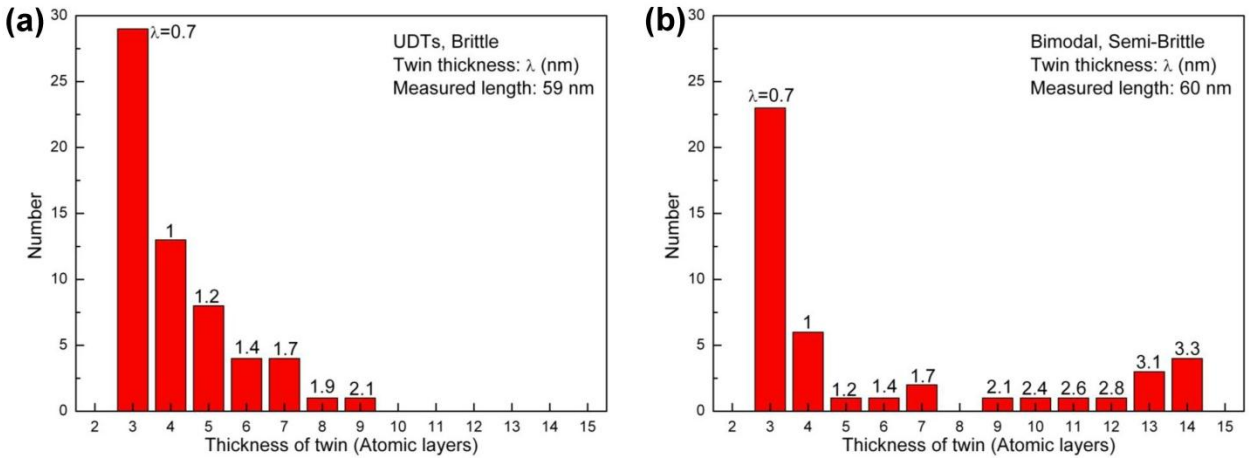

Supplementary Figure S1: Two examples of statistical twin distributions in ultra-twinned Au nanowires (NWs) with distinct fracture modes. . (a) The NW with ultrahigh density twins (UDTs) was made of twins less than 2.1 nm in thickness with a predominance of twins at the minimum limit of 0.7 nm and exhibited brittle-like fracture. **(b)** The NW with bimodal twin distribution showed a mixture twin spacing with UDTs and low density twins (LDTs) and exhibited semi-brittle fracture.

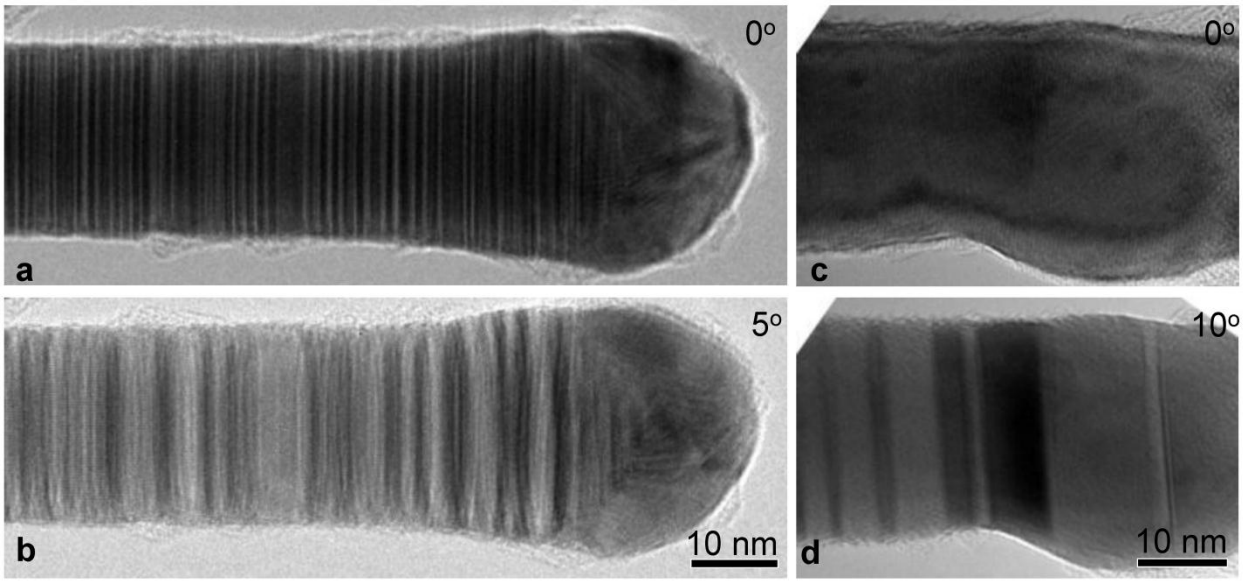

Supplementary Figure S2: Twin morphology of Au NWs at different tilt angle. (a) Au NWs with UDTs in [110] zone axis. **(b)** After a tilt of 5^{o} along α direction, the NW presents as bamboo-like structure with less visible UDTs. **(c-d)** The Au NW shows no twin boundary (TB) at 0^{o}. However, several TBs appear after a tilt of 10^{o} along α direction (d). Both of (c) and (d) are not taken perfectly in the [110] zone axis, but more TBs could show up when aligned closer to the [110] zone axis.

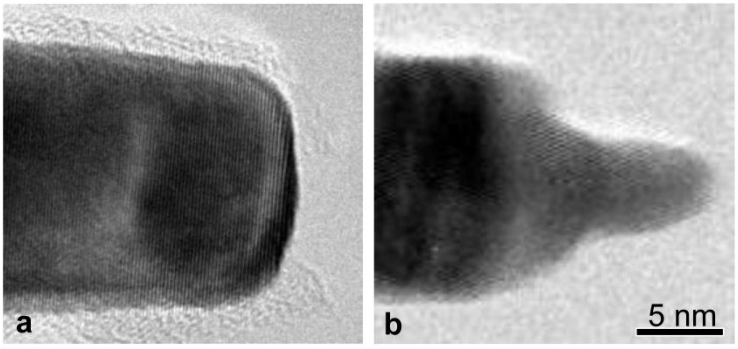

Supplementary Figure S3: Two types of fracture modes observed in ultra-twinned Au NWs. (a) Brittle-like fracture with a flat fracture surface observed in the sample with UDTs in Fig. 1c-d. **(b)** Semi-brittle fracture with a tiny tip in the fracture zone observed in the sample with bimodal structure in Fig. 1c-d.

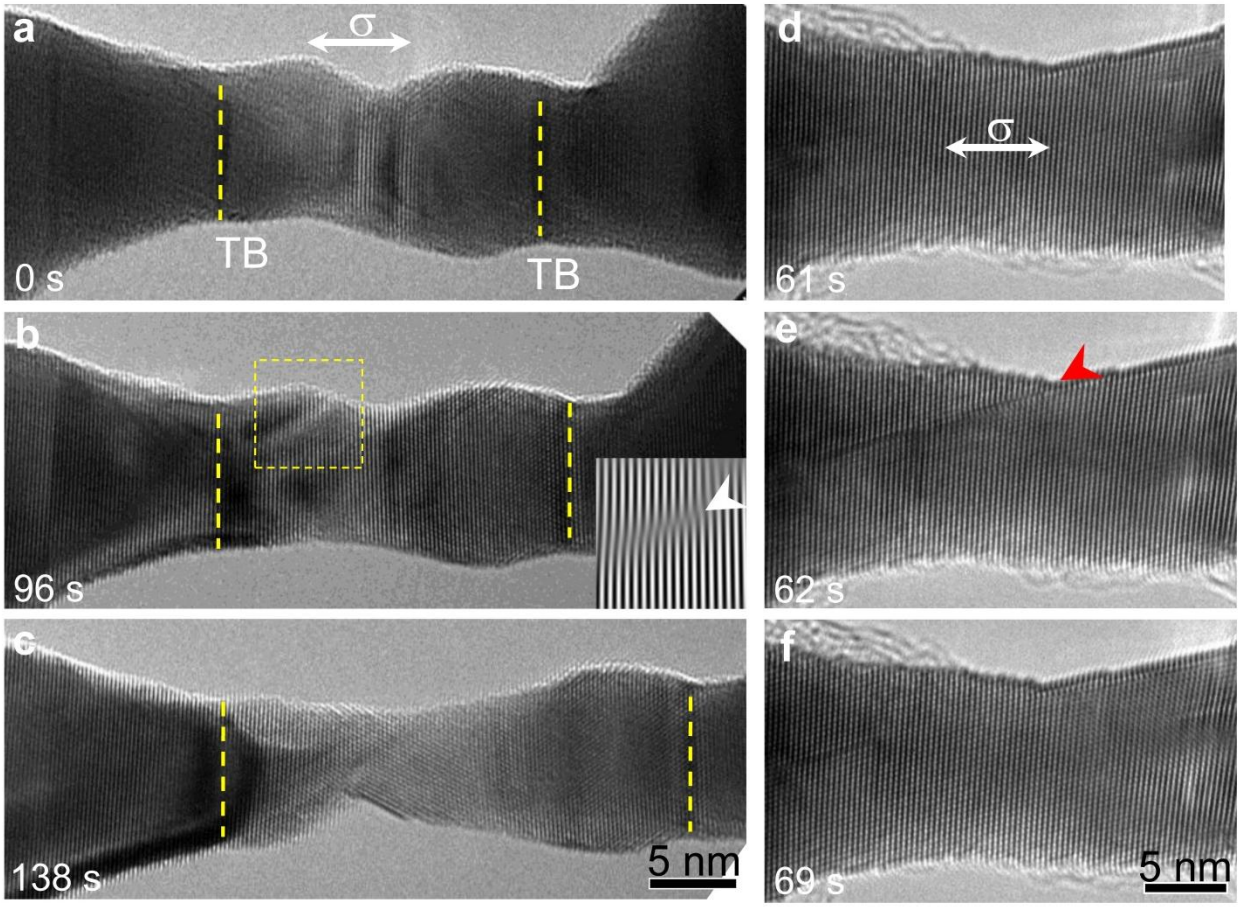

Supplementary Figure S4: Process of ductile fracture in Au NWs with LDTs (λ > 5.6 nm) and no twins. (a) TEM image of a pristine Au NW with LDTs created by cold welding technique. TBs are marked out by a dash line in yellow color. **(b)** During tensile loading, the NW is elongated purely elastically then yields plastically by heterogeneous nucleation of partial dislocations from the free surface. An inverse FFT image of surface-nucleated dislocation is shown in inset. **(c)** Formation of extended necking between two TBs before fracture. **(d-f)** The deformation of Au NW with no twins is dominated by the surface emission of partial dislocations, similar to the deformation of Au NWs with LDTs. However, in Au NWs with LDTs, TBs serve as barriers to the motion of partial dislocations, contributing to the observed strain hardening effect.

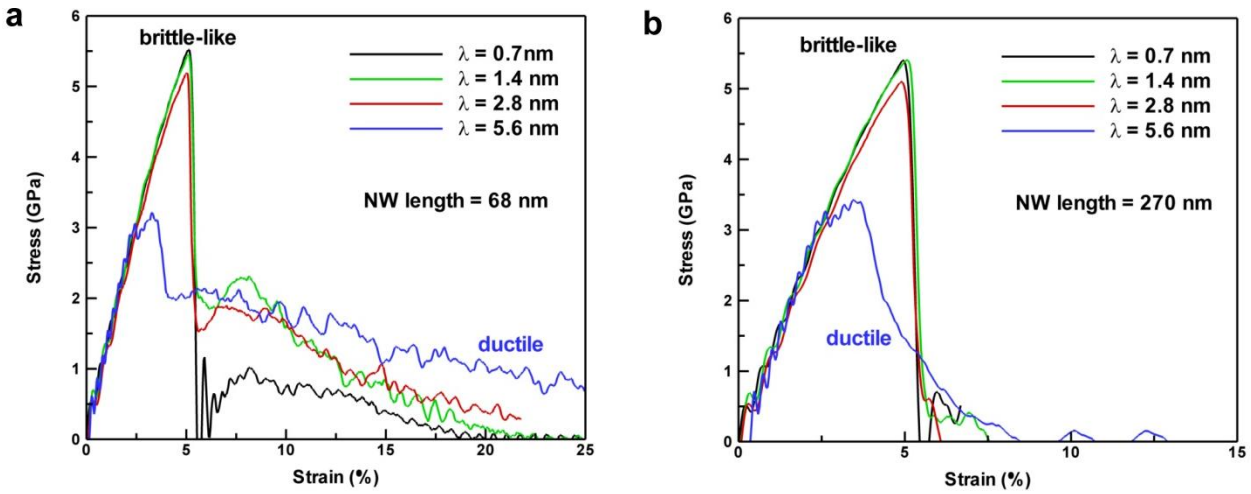

Supplementary Figure S5: Stress-strain curves of ultra-twinned Au NWs computed from molecular dynamics (MD) simulations as a function of twin thickness (λ). All models have uniform twin distribution. The NW periodic length is 68 nm in **(a)** and 270 nm in **(b)**.

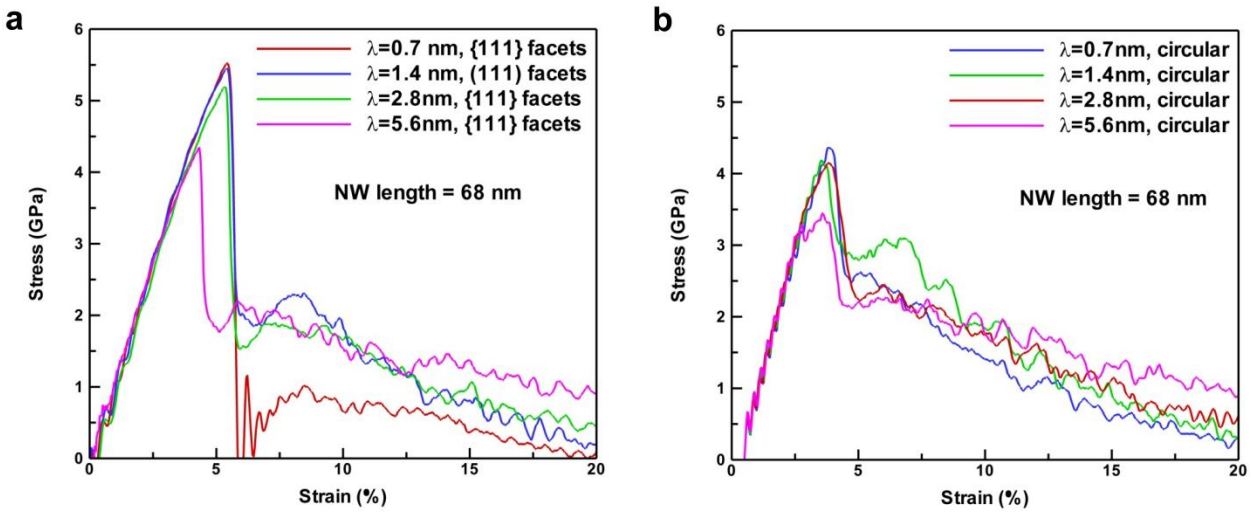

Supplementary Figure S6: Effects of surface structure on stress-strain curves of ultra-twinned Au NWs computed from MD simulations for different λ. (a) Surface morphology with {111} microfaceting. **(b)** Perfectly circular surface structure.

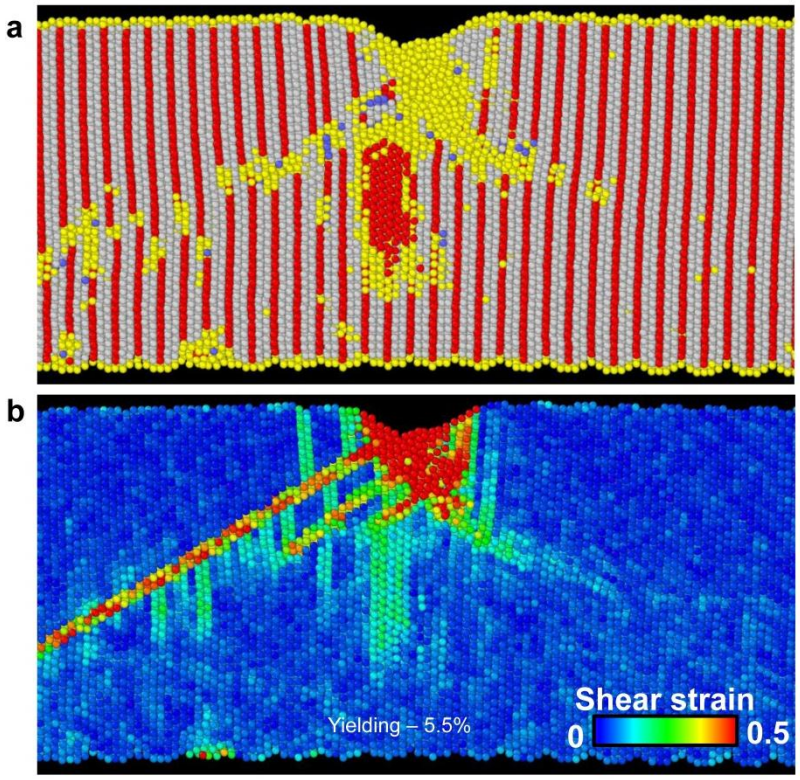

Supplementary Figure S7: MD computer simulation of local crystal structure and shear strain in a brittle-like ultra-twinned Au NW with λ = 0.7 nm and {111} surface faceting. (a) The deformation snapshot at the yielding point. **(b)** Corresponding map of atomic-scale shear strain showing a highly-localized shear zone. Even at the yielding point, the local UDTs are unstructured and shear localization induced necking already forms, which clearly demonstrates that the tendency of brittle fracture is further promoted by decreasing λ to the limit.

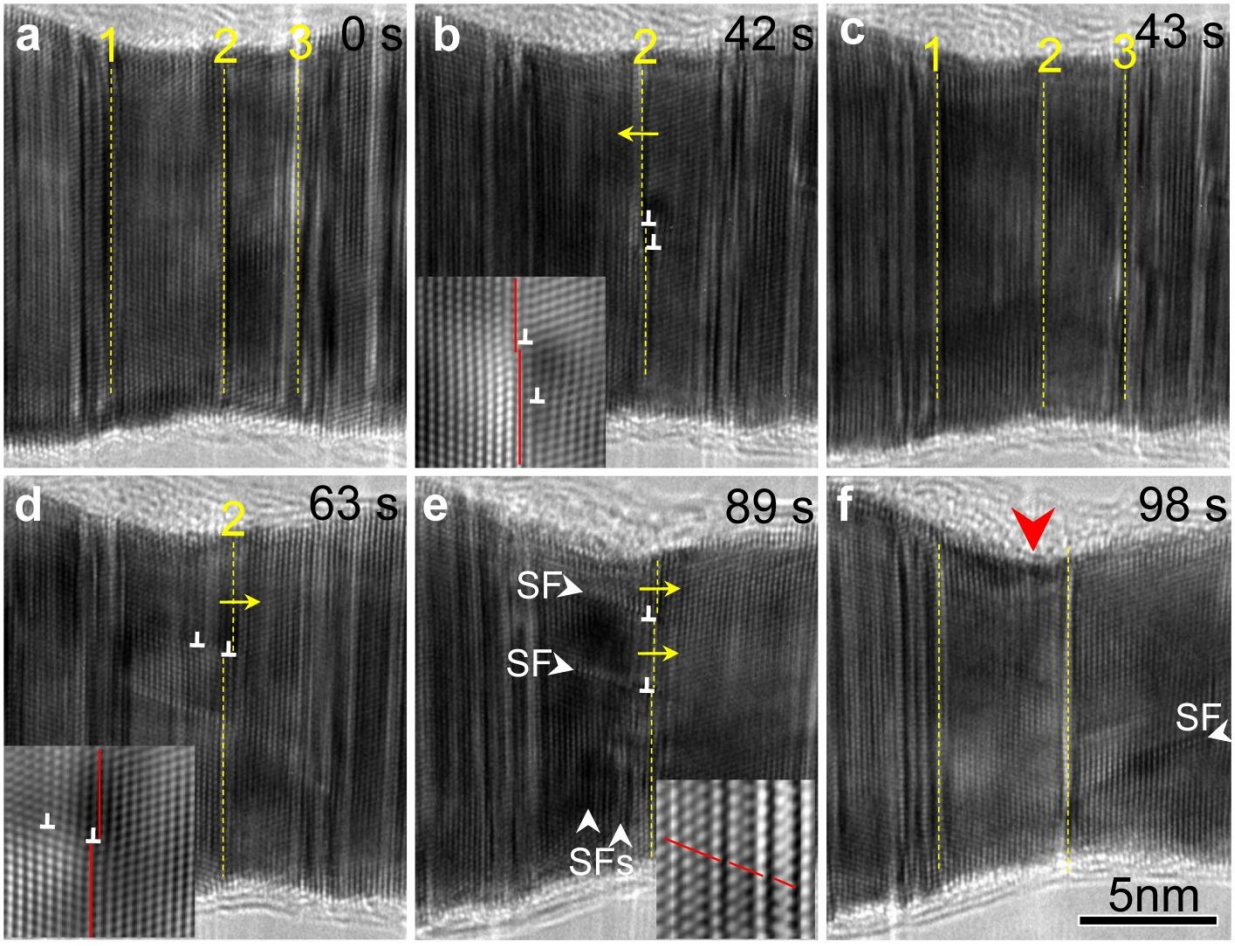

Supplementary Figure S8: Sequential images showing the de-twinning and necking process in a semi-brittle Au NWs with bimodal twin structures. (a) Pristine Au NW with bimodal twin structures. The deformation mainly occurs at the part with larger λ, as marked out by dash lines in yellow from TB_1 to TB_3. **(b-d)** Dislocations nucleate homogeneously in the part with larger λ, propagate and are blocked by the TB_2, which produce atomic ledges to TB_2 and finally induce the TB_2 migration. The inset in (b) and (d) are the inverse FFT images showing the dislocations blocked by TB_2. **(e-f)** The propagation of stacking faults (SFs) parallel to the twin plane accompanied with necking formation. Inset shows the structure of SFs. The red arrow points out the localized necking.

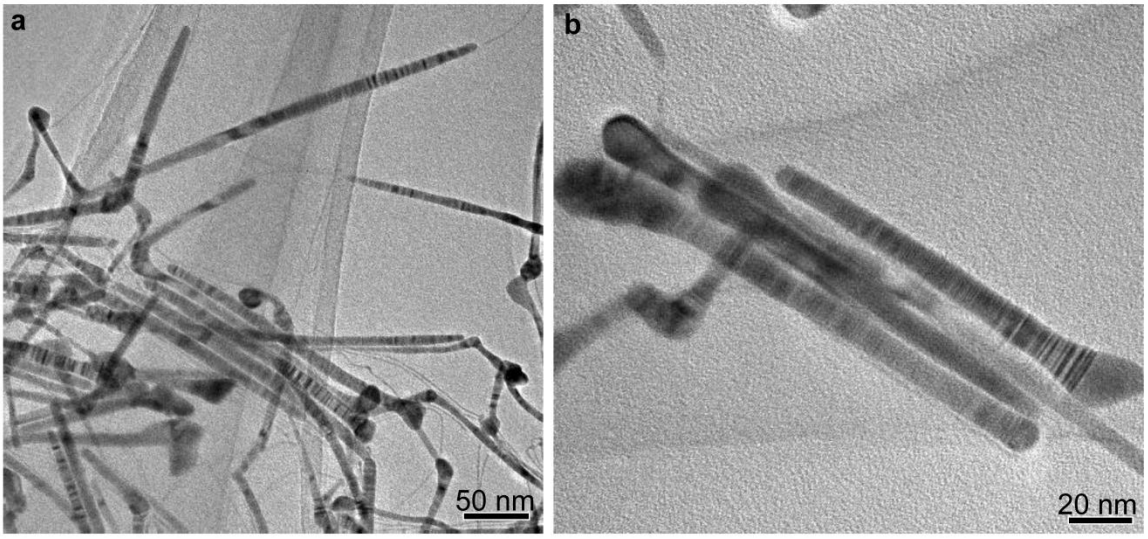

Supplementary Figure S9: Representative morphology of as-synthesized Au NWs with ultra-twins by TEM. The diameter of Au NWs presented in our study was mostly uniform along the axial direction. Some variations in diameter were only observed at the two ends of the NWs, which did not significantly affect the stress-strain measurements.